

文章编号 2097-1842(2025)04-0921-10

Arbitrary azimuthal optical field manipulation by dual-spiral arrays

MA Li*, WANG Ying, LI Min, ZHANG Ying, ZHAO Bo*

(Department of Physics, Changzhi University, Changzhi 046011, China)

* Corresponding author, E-mail: mali9001@126.com; zy828522@163.com

Abstract: Optical field manipulation, an emerging frontier in photonics, demonstrates significant potential in biomedical microscopy, quantum state engineering, and micro-nano fabrication. To address the critical limitations of current optical modulation technologies in achieving full-parameter precision control, we proposed a novel approach for dynamic azimuthal optical field modulation based on dual-spiral arrays. By designing spatially interleaved spiral structures with different initial radii while maintaining identical periodic parameters, we achieved continuous optical modulation spanning the full $0-2\pi$ range in azimuthal field distribution. Through rigorous numerical simulations, we systematically established a quantitative correlation between the structural parameters and azimuthal optical field patterns, revealing, for the first time, a quasi-linear relationship between the radius difference and the resultant optical distribution. This theoretical framework advances our fundamental understanding of structured optical field manipulation as well as provides a new paradigm for programmable photonic device design, with distinct technical advantages in super-resolution imaging and optical tweezer systems.

Key words: optical manipulation; topological charge; spiral array

基于双螺旋阵列的光场任意角向调控

马力*, 王颖, 李敏, 章颖, 赵波*

(长治学院物理系, 山西长治 046011)

摘要: 光场调控作为现代光子学的前沿研究方向, 在生物医学显微成像、量子态操控及微纳制造等领域展现出重要应用价值。本研究针对现有光场调控技术在全参量精密操控维度受限的关键问题, 提出基于双螺旋阵列的方位角光场

收稿日期: 2025-02-07; 修订日期: 2025-03-03

基金项目: 山西省基础研究计划项目 (No. 202403021212017); 山西省高等学校科技创新项目 (No. 2024L349, No. 2022L513); 长治市技术创新中心项目 (No. 2022cx002) 资助; 光伏技术与应用山西省重点实验室 (山西潞安太阳能科技有限责任公司) 开放基金 (No. SXKL2024-05)

Supported by Applied Basic Research Project of Shanxi Province (No. 202403021212017); Scientific and Technological Innovation Programs of Higher Education Institutions in Shanxi (STIP) (No. 2024L349, No. 2022L513); Technology Innovation Center Program of Changzhi (No. 2022cx002); Shanxi Key Laboratory of Photovoltaic Technology and Applications (Shanxi Lu'an Solar Energy Technology Co., Ltd.) (No. SXKL2024-05)

动态调制新方法。通过构建具有差异化初始半径参数的空间交错螺旋结构,在保持周期参数一致性的前提下,实现了光场方位角分布从 0 到 2π 范围的连续光场调制。基于严格数值仿真,系统解析了双螺旋阵列结构参数与方位角光场分布的映射规律,揭示了螺旋半径差与方位角分布间的准线性对应关系。该理论模型不仅深化了空间结构光场调控的物理认知,更为可编程光学器件设计提供新的技术路径,在超分辨成像和光学镊子等应用场景中展现出显著的技术优势。

关键词:光场调控;拓扑荷;螺旋阵列

中图分类号:O0436.1

文献标志码:A

doi:10.37188/CO.EN-2025-0007

CSTR:32171.14.CO.EN-2025-0007

1 Introduction

Optical field manipulation, a fundamental branch of modern optical research, focuses on the precise control of light propagation characteristics, including phase, amplitude, and polarization states^[1]. This technology has been applied extensively in various fields. In optical communications^[2], optical field manipulation significantly enhances bandwidth and transmission efficiency, driving advancements in information technology to meet the ever-growing data demands^[3]. In microscopy and imaging systems^[4], the manipulation of optical fields enhances resolution and contrast, driving progress in high-precision imaging technologies^[5]. Furthermore, the precise control of optical fields enables micromachining of materials and laser fabrication, which have substantial applications in the manufacturing sector^[6-7]. Optical field manipulation can also enhance the quality and characteristics of laser beams by enabling the generation of ultrashort pulse lasers^[8], thereby fostering innovation in laser technology^[9]. In terms of application prospects, research on optical field manipulation is evolving toward intelligent optical systems^[10], focusing on the development of adaptive optical devices that achieve real-time manipulation of optical fields, thus enhancing the flexibility and responsiveness of optical systems^[11-12]. In the field of nano-optics^[13-15], researchers are exploring the fine control of optical fields at the nanoscale for applications in optical information processing and sensor technologies, with the aim of enhancing system performance^[16-17]. The integration of optical field manipulation with quantum

optical technology facilitates the preparation and detection of quantum states, thereby advancing the field of quantum information science^[18-19]. Moreover, the development of advanced biological imaging technologies enables non-invasive detection and diagnostics^[20-21], ultimately improving the precision and efficiency of medical imaging^[22-24]. In summary, advancements in optical field manipulation provide new directions for modern optical research as well as open up broader possibilities in related application fields.

In recent years, the arbitrary azimuthal manipulation of optical fields has emerged as a crucial technique in optics, demonstrating immense potential for applications involving complex optical fields and higher-order optical fields. Arbitrary directional manipulation of optical fields involves not only the adjustment of traditional optical characteristics but also holistic control of the spatial distribution of light, phase structures^[25], and their interactions with matter^[26]. Spatial light modulators (SLMs) are extensively employed in optical field manipulation. By designing optical elements, SLMs enable real-time control over the phase and amplitude of light, facilitating precise adjustments to the divergence angle and transmission modes of optical fields^[27-28]. For instance, liquid-crystal SLMs can generate various beam structures, such as vortices and honeycomb beams, thereby realizing multi-directional control. The optical phase array technology enables the arbitrary reconstruction of optical wavefronts^[29]. The desired optical field could be generated at any angle by adjusting the phase of each element in the array. The integration of this technology offers new design concepts for miniaturized optical devices, such as

intelligent LiDAR and optical communication equipment^[30]. Computational optics further enhance the complex optical field structures through numerical calculations and algorithmic adjustments^[31-32]. Techniques such as digital holography theoretically enable arbitrary directional manipulation and offer significant applications in optical imaging and optic capturing. Furthermore, nonlinear optical effects, such as four-wave mixing and self-focusing, enable researchers to achieve arbitrary directional enhancement and control of optical fields^[33-34]. These nonlinear effects not only change the direction of light propagation but also modulate the properties of light, providing new avenues for optical field manipulation. The development of smart materials and adaptive optics technologies has enhanced the flexibility and immediacy of optical field manipulation. These technologies can automatically adjust the propagation direction and mode of light in response to changes in the external environment, thereby significantly improving the adaptability and functionality of optical fields. Despite significant advancements in the arbitrary azimuthal manipulation of optical fields, several challenges remain. The key issues include achieving more efficient spatial control over optical fields and integrating optical field manipulation technologies into compact devices to improve their practicality.

In this study, we propose dual-spiral arrays composed of two interleaved spiral arrays to achieve modulations of azimuthal optical fields. These arrays differed in their initial radii, whereas all other parameters remained unchanged. By precisely tuning the difference in radius between the two spiral structures, we achieved continuous control over the azimuthal field distribution. To gain deeper insight into the azimuthal distribution of the dual-spiral array structure, we performed numerical simulations. Through systematic analysis, we examined the relationship between the structural characteristics of the dual-spiral arrays and the resulting azimuthal optical field distribution. The simulation results demon-

strate that, by accurately controlling the radius difference between the two arrays, the azimuth of the optical field can be smoothly varied across the entire range from 0 to 2π . Furthermore, we observed a nearly linear correlation between the radius difference and the azimuthal distribution, offering valuable insights for the design and optimization of optical devices based on this structure.

2 Principle and method

Figure 1(a) (color online) schematically illustrates the modulation model of the dual-spiral arrays. Defined in polar coordinates (r, θ) , the dual-spiral arrays can be expressed as

$$\begin{aligned} r_1 &= -\left[r_{10} + \frac{lz\lambda}{2\pi r_{10}} (\pi - \theta) \right] \\ r_2 &= r_{20} + \frac{lz\lambda}{2\pi r_{20}} \theta \end{aligned} \quad (1)$$

where r_{10} and r_{20} are the initial radii, l indicates the topological charge, z denotes the diffraction distance, and λ indicates the wavelength. Owing to the counter rotational structure and mirror-symmetric configuration of the dual-spiral arrays, the spiral r_1 is assigned a negative coordinate accompanied by an azimuthal transformation of $\pi - \theta$. The modulation of the transmitted optical field is fundamentally governed by the parametric dependence of the spiral radius r variation with respect to the azimuthal angle θ . As the beam passes through this dual-spiral structure, the spirals introduce a specific phase delay in the light perpendicular to the wavefront. Various phase distributions can be obtained by adjusting the topological charges of the spirals. The combination of these distinct phase shifts and amplitude variations collectively formed a helical phase structure. The interaction of the two helical phase fronts from the spirals, along with the modulation effects of the constructive and destructive interference, resulted in an optical field that exhibited two focal spots surrounding a central zero-intensity distribution, as shown in Fig. 1(c).

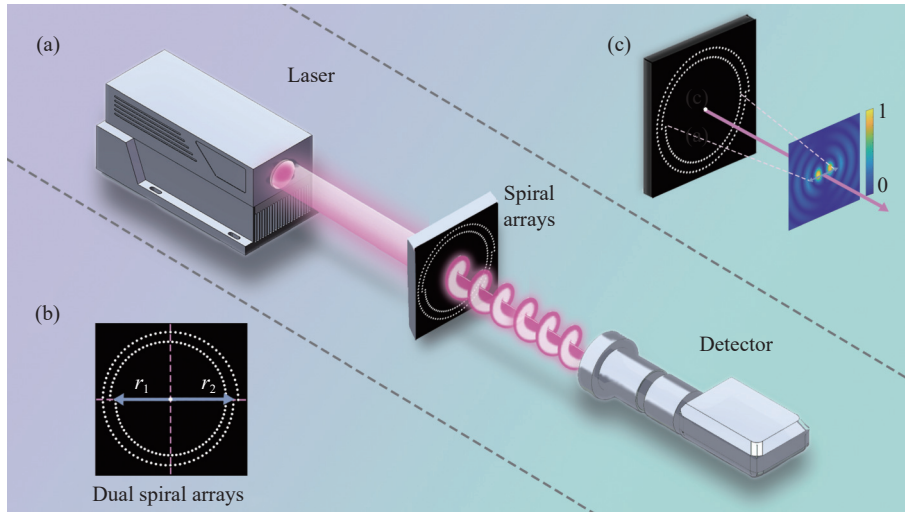


Fig. 1 Schematic model of the optical field manipulation based on the dual-spiral arrays. (a) Model setup, consisting of a laser, dual-spiral arrays, and a detector. (b) Front view of the dual-spiral arrays. The dual-spiral arrays are composed of an inner spiral and an outer spiral, with each spiral consisting of multiple pinholes represented by white dots. The blue arrows indicate the radii of the spirals, denoted as r_1 and r_2 , respectively. (c) Intensity field generated by the dual-spiral arrays

Figure 1(b) shows a front view of the dual-spiral arrays. These arrays consisted of two interleaved spiral structures with both the inner and outer spirals composed of multiple pinholes. The inner spiral exhibited a right-handed orientation, whereas the outer spiral was left-handed, with the rotational directions demonstrating mirror symmetry. The mirror-symmetric configuration of the dual-spiral arrays facilitated complementary phase modulations within the optical field, resulting in petal-like intensity distributions through the interplay between the constructive and destructive interference effects. The modulation mechanism of the dual-spiral arrays involves precise control over both the phase and amplitude of the light, enabling the modulation of the optical field to achieve specific azimuthal characteristics.

For this operational mode, we set the wavelength to 1550 nm, the propagation distance to 1 m, the initial radius of each spiral array to 5 mm, the radius of pinholes to 30 μm , and the number of pinholes to 100. Once the number of pinholes reached a threshold sufficient to form a uniform spiral, any further increase in the number of pinholes had a negligible effect on the optical field characteristics

and phase distribution. The structural parameters of the dual-spiral configuration were strategically optimized to ensure practical feasibility for future experimental implementations. The initial radius of the spiral arrays was chosen to accommodate both the number and size of the pinholes to achieve an optimal spatial distribution within the azimuthal periodicity of the spiral. The pinhole dimensions were determined based on the achievable fabrication precision and tolerance in femtosecond laser micromachining. In addition, the operational wavelength is strategically aligned with standard telecommunications to facilitate future practical applications in optical communication. Keeping the aforementioned parameters fixed, we varied the radius difference and topological charge of the dual spirals to investigate their influence on the optical field characteristics and phase distribution of multiple beams.

3 Simulation and discussion

3.1 Dual-spiral arrays with the first-order topological charge

Figure 2(a) (color online) shows dual-spiral arrays with varying radial differences between the in-

ner and outer spirals, denoted by the variable Δr_3 at the center of the figure. Specifically, the radius difference is defined as the arithmetic difference between their respective initial radii, mathematically expressed as $\Delta r = r_{20} - r_{10}$. The gray arrows on the outer circle indicate the direction of rotation, whereas the numbers within the arrows correspond to the radial differences of the dual-spiral arrays. The radius differences are selected uniformly within the range of $10 \mu\text{m}$ to $250 \mu\text{m}$. As the radius difference increases from (a1) to (a12) in Fig. 2, the inner spiral contracts progressively inward. Initially, in (a1), the inner spiral nearly coincides with the outer

spiral. The corresponding intensity distributions of the dual-spiral arrays in Fig. 2(b) (color online) exhibit two focal spots surrounding the central zero-intensity region. Central phase distribution displays uniform and singularity-free equiphase lines with phase jumps forming a pattern of two semicircles. By continuously adjusting the radius difference between the two spirals, the resulting intensity and phase distributions can be smoothly rotated. However, despite the changes in the radius difference, the overall profiles of the intensity and phase distributions remained consistent, as clearly illustrated in Fig. 2.

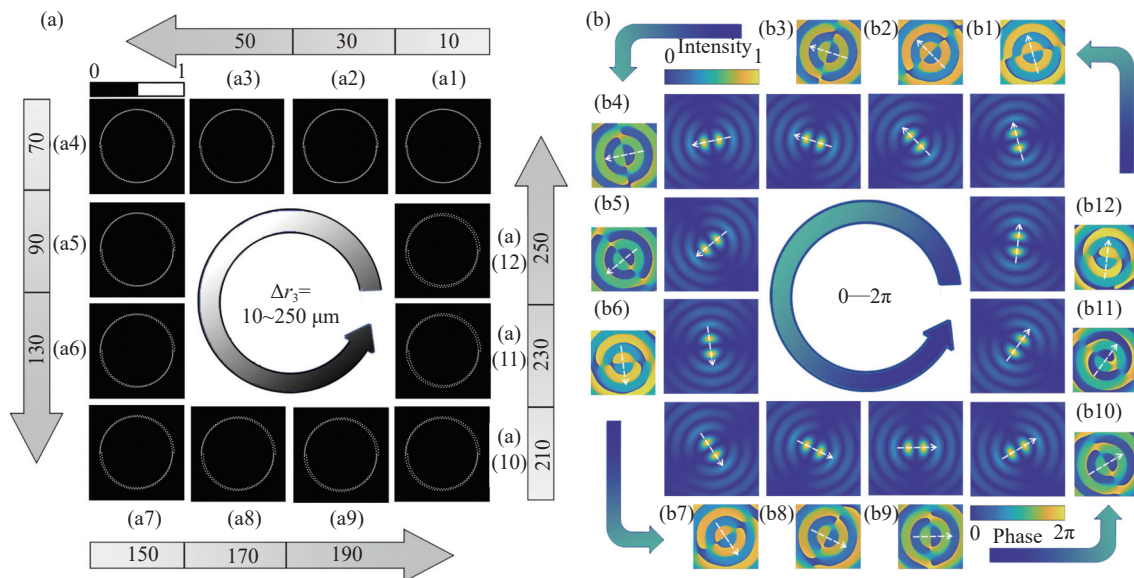


Fig. 2 Schematic of the optical field modulated by dual-spiral arrays with first-order topological charges. (a) Structures of dual-spiral arrays, each characterized by varying spiral radii. (b) Sequentially presents the intensity and phase distributions progressing from the inner to the outer layer. Sequences (a1)–(a12) and (b1)–(b12) correspond in terms of the arrangement direction, collectively showcasing 12 datasets with different spiral radius variations linked to intensity and phase distributions. Each set of images rotates according to the directions indicated by the arrows on the inner and outer circles. In the intensity and phase distribution maps shown in (b), the white dotted arrows denote the azimuthal direction of the optical field

3.2 Dual-spiral arrays with the third-order topological charge

Similar to Fig. 2(a), Fig. 3(a) (color online) depicts dual-spiral arrays with varying radius differences, where the spirals are assigned a topological charge of 3. The radius difference between the inner and outer spirals is denoted by the variable Δr_4 . The gray arrows on the outer circle indicate the direction of rotation, with the numbers inside the arrows corresponding to the respective radius differences of the dual-spiral arrays. As the radius difference increases from (a1) to (a12) in Fig. 3, the inner spiral contracts progressively inward. Fig. 3(b) (color online) shows that the modulation of the dual-spiral arrays, which carry a third-order topological charge, results in an intensity distribution character-

ization of rotation, with the numbers inside the arrows corresponding to the respective radius differences of the dual-spiral arrays. As the radius difference increases from (a1) to (a12) in Fig. 3, the inner spiral contracts progressively inward. Fig. 3(b) (color online) shows that the modulation of the dual-spiral arrays, which carry a third-order topological charge, results in an intensity distribution character-

ized by a six-petal flower-like symmetry surrounding a central dark spot. The central phase distribution rotates continuously from 0 to 6π over the full azimuthal cycle. Radius differences are selected uniformly, ranging from 10 μm to 850 μm , facilitating

a continuous rotation of both intensity and phase distributions. Moreover, modifying the radius difference alone does not affect the shapes of the intensity and phase distributions, which is a feature similar to the observations shown in Fig. 2.

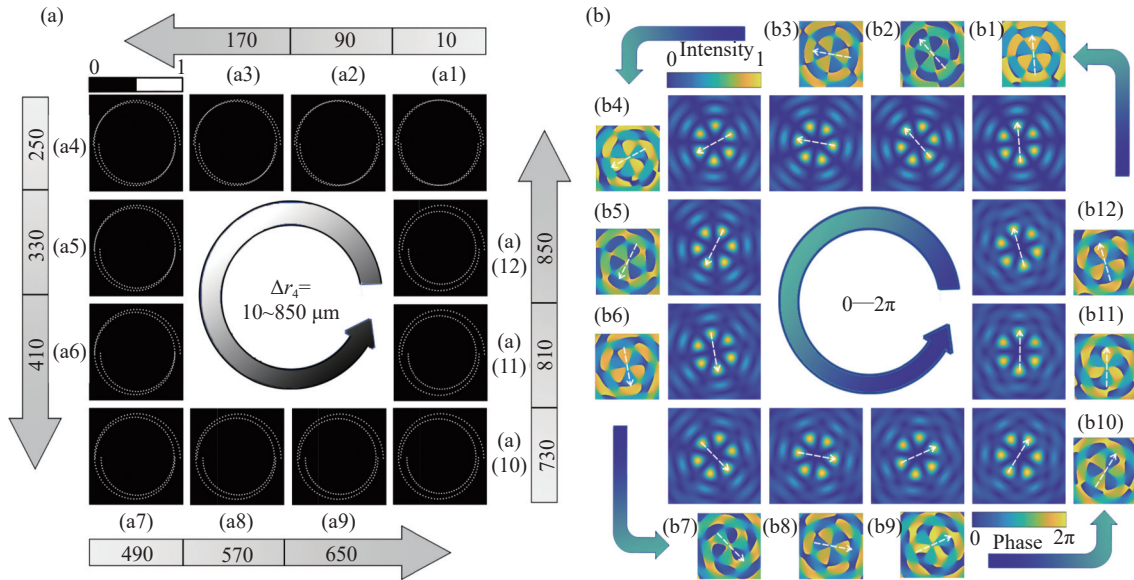


Fig. 3 Schematic of the optical field modulated by dual-spiral arrays with third-order topological charges. (a) Structures of dual-spiral arrays with different spiral radii. (b) Sequentially presents the intensity and phase distributions progressing from the inner to the outer layer. The images in (a1)–(a12) and (b1)–(b12) are arranged in the corresponding directions, collectively displaying 12 datasets with different spiral radius differences and their corresponding intensity and phase distributions. Each set of images rotates according to the directions indicated by the arrows on the inner and outer circles. In the intensity and phase distribution maps shown in (b), the white dotted arrows denote the azimuthal direction of the optical field

In summary, the numerical simulation analyses presented in Figs. 2 and 3 indicate that when the inner and outer spirals share the same order of topological charge, adjusting the radius difference between the two spirals enables precise control of the azimuthal variation of the generated optical field. A comparison between Figs. 2 and 3 further reveals that, as the topological charge of the dual-spiral arrays increases from the first to the third order, a greater radius difference is required for the azimuthal angle of the optical field to complete a full rotation. Notably, the petal-like intensity profile of the generated optical field was deformed and eventually deteriorated as the topological charge increased to higher orders. This phenomenon arises from the inherent structural asymmetry of a single-

spiral configuration. As the topological charge l increases, the expanding radial variation of the spiral induces a deviation from circular symmetry, preventing the formation of the expected intensity profile^[35-36].

However, parameter adjustments can be applied to achieve the desired modulation effect. Specifically, as the topological charge l increases, reducing the diffraction distance z aids in maintaining the modulation effect of the spiral structure. The supplementary file provides additional data and figures illustrating the azimuthal optical modulations for topological charges $l = 6$ and $l = 9$.

3.3 Relationship between radius differences and azimuthal optical field

Based on the above analysis, we extracted data

on azimuthal angles and spiral radius differences to investigate their specific relationships. Figure 4(a) (color online) presents a comparative analysis of the azimuthal optical field as a function of the difference in radii. The purple and blue linear fit lines, corresponding to spiral topological charges of $l = 1$ and $l = 3$, respectively, exhibit a quasi-linear relationship between Δr and azimuthal angle. Figures 4(b) and 4(c) (color online) display the corresponding sector plots. The results reveal the fol-

lowing principles: First, varying the radius difference of the dual-spiral arrays enables azimuthal manipulation of the optical field over a full 0 to 2π range. Second, the relationship between the radius differences and azimuth exhibited a quasi-linear variation. Third, for the same radius difference in the dual-spiral arrays, different topological charges lead to varying amplitudes of the azimuthal variation in the optical field, with the amplitude decreasing as the topological charge increases.

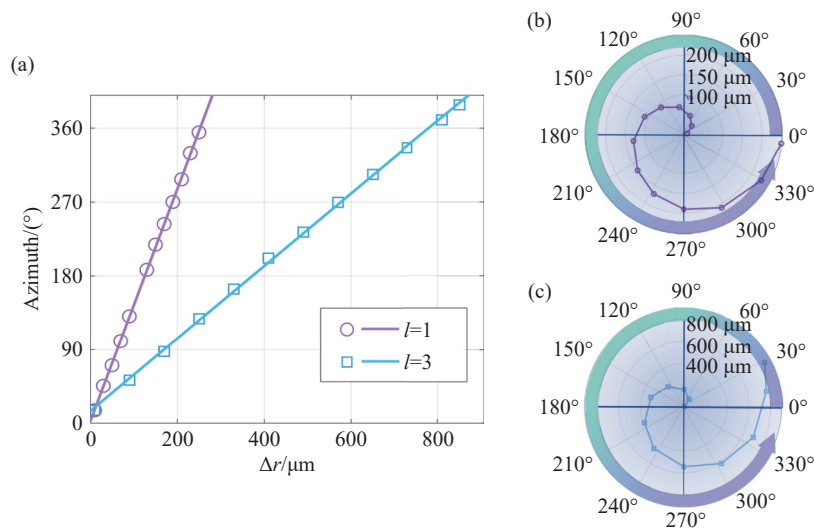


Fig. 4 (a) Radial difference of the dual-spiral arrays as a function of the azimuthal angle of the optical field, with the linear fit lines of the purple line representing spirals with a first-order topological charge and the blue line representing spirals with a third-order topological charge. (b) and (c) show the sector plots of the azimuthal variation of the optical field for topological charges $l = 1$ and $l = 3$, respectively, with sector plots spanning from 0° to 360°

This study reveals that the radius disparity between the dual-spiral arrays plays a crucial role in the azimuthal manipulation of the optical field. The stabilities of the intensity and phase distributions indicate that the generated optical field maintained a consistent profile. These findings provide a theoretical foundation for the precise control of azimuthal optical field manipulation, which is of considerable importance for flexible steering of optical fields. Drawing on the modulation principle of dual-spiral arrays, which induce a phase gradient through radial differences, any phase-modulated approach that conforms to spiral phase profile encoding can be employed to achieve precise azimuthal control of the optical field. For example, liquid crystals, which

are excellent phase-encoded modulators owing to their exceptional electro-optic tunability and high-resolution phase modulation, play a vital role in optical control. Recent advancements in the dynamic control of optical vortices and complex wavefronts have further demonstrated their significance in optical field manipulation^[37-39].

4 Conclusion

This paper introduces the concept of dual-spiral arrays, comprising two interleaved spiral arrays designed to manipulate the azimuthal optical field. These arrays were distinguished solely by their initial radii, with all the other parameters remaining

constant. By precisely controlling the radius difference between the two spiral configurations, the azimuthal distribution of the optical field can be continuously adjusted. To better understand how the dual-spiral array structure influences the azimuthal distribution, we conducted numerical simulations. Through comprehensive analysis, we investigated the relationship between the structural characteristics of the dual-spiral arrays and the resulting azimuthal optical field distribution. The simulation results reveal that by accurately controlling the radius difference, the azimuth of the optical field can be

continuously varied across the full range from 0 to 2π . Furthermore, we observed a quasi-linear correlation between the radius difference and the azimuthal distribution, indicating that changes in the radius difference produced nearly proportional adjustments to the azimuthal distribution of the optical field. These findings provide valuable insights into the manipulation of optical fields, potentially paving the way for new applications in fields such as optical communication, microscopy, and optical trapping, where the precise control of the azimuthal optical field is crucial.

References:

- [1] DHOLAKIA K, ČIŽMÁR T. Shaping the future of manipulation[J]. *Nature Photonics*, 2011, 5(6): 335-342.
- [2] LIU W W, LI ZH CH, ANSARI M A, *et al.*. Design strategies and applications of dimensional optical field manipulation based on metasurfaces[J]. *Advanced Materials*, 2023, 35(30): 2208884.
- [3] LIU CH B, BAI Y, ZHAO Q, *et al.*. Fully controllable Pancharatnam-Berry metasurface array with high conversion efficiency and broad bandwidth[J]. *Scientific Reports*, 2016, 6(1): 34819.
- [4] MAURER P C, MAZE J R, STANWIX P L, *et al.*. Far-field optical imaging and manipulation of individual spins with nanoscale resolution[J]. *Nature Physics*, 2010, 6(11): 912-918.
- [5] PAN M Y, FU Y F, ZHENG M J, *et al.*. Dielectric metalens for miniaturized imaging systems: progress and challenges[J]. *Light: Science & Applications*, 2022, 11(1): 195.
- [6] MA Q J, REN G H, XU K, *et al.*. Tunable optical properties of 2D materials and their applications[J]. *Advanced Optical Materials*, 2021, 9(2): 2001313.
- [7] HAZZAN K E, PACELLA M, SEE T L. Laser processing of hard and ultra-hard materials for micro-machining and surface engineering applications[J]. *Micromachines*, 2021, 12(8): 895.
- [8] HAN M L, SMITH D, NG S H, *et al.*. Ultra-short-pulse lasers—materials—applications[J]. *Engineering Proceedings*, 2021, 11(1): 44.
- [9] MINCUZZI G, GEMINI L, FAUCON M, *et al.*. Extending ultra-short pulse laser texturing over large area[J]. *Applied Surface Science*, 2016, 386: 65-71.
- [10] MATA J, DE MIGUEL I, DURÁN R J, *et al.*. Artificial intelligence (AI) methods in optical networks: a comprehensive survey[J]. *Optical Switching and Networking*, 2018, 28: 43-57.
- [11] HAMPSON K M, TURCOTTE R, MILLER D T, *et al.*. Adaptive optics for high-resolution imaging[J]. *Nature Reviews Methods Primers*, 2021, 1(1): 68.
- [12] MOCCI J, QUINTAVALLA M, TRESTINO C, *et al.*. A multiplatform CPU-based architecture for cost-effective adaptive optics systems[J]. *IEEE Transactions on Industrial Informatics*, 2018, 14(10): 4431-4439.
- [13] ZAYATS A V, SMOLYANINOV I I, MARADUDIN A A. Nano-optics of surface plasmon polaritons[J]. *Physics Reports*, 2005, 408(3-4): 131-314.
- [14] ZHANG Q, HU G W, MA W L, *et al.*. Interface nano-optics with van der Waals polaritons[J]. *Nature*, 2021, 597(7875): 187-195.
- [15] TSENG E, COLBURN S, WHITEHEAD J, *et al.*. Neural nano-optics for high-quality thin lens imaging[J]. *Nature Communications*, 2021, 12(1): 6493.
- [16] WANG H L, YOU E M, PANNEERSELVAM R, *et al.*. Advances of surface-enhanced Raman and IR spectroscopies: from nano/microstructures to macro-optical design[J]. *Light: Science & Applications*, 2021, 10(1): 161.
- [17] DE KONINCK Y, CAER C, YUDISTIRA D, *et al.*. GaAs nano-ridge laser diodes fully fabricated in a 300-mm cmos

- pilot line[J]. *Nature*, 2025, 637(8044): 63-69.
- [18] WALMSLEY I A. Quantum optics: science and technology in a new light[J]. *Science*, 2015, 348(6234): 525-530.
- [19] DOWLING J P, SESHADREESAN K P. Quantum optical technologies for metrology, sensing, and imaging[J]. *Journal of Lightwave Technology*, 2015, 33(12): 2359-2370.
- [20] XIA CH X, CHENG H M, HOU X W, *et al.*. Spherical nucleic acids for biomedical applications[J]. *Advanced Sensor and Energy Materials*, 2024, 3(4): 100117.
- [21] HASHEMITAHERI M, EBRAHIMI E, DE SILVA G, *et al.*. Optical sensor for BTEX detection: integrating machine learning for enhanced sensing[J]. *Advanced Sensor and Energy Materials*, 2024, 3(3): 100114.
- [22] NTZIACHRISTOS V. Going deeper than microscopy: the optical imaging frontier in biology[J]. *Nature Methods*, 2010, 7(8): 603-614.
- [23] 陈瀑, 杨健, 褚小立, 等. 近五年我国近红外光谱分析技术的研究与应用进展[J]. 分析化学, 2024, 52(9): 1213-1224.
- CHEN P, YANG J, CHU X L, *et al.*. Research and application progress of near infrared spectroscopy analytical technology in China in the past five years[J]. *Chinese Journal of Analytical Chemistry*, 2024, 52(9): 1213-1224. (in Chinese).
- [24] 邢蕾, 牟含章, 潘建斌, 等. 真空紫外激光解吸/电离单细胞质谱成像装置的研制和调试[J]. 应用化学, 2024, 41(1): 100-108.
- XING L, MOU H Z, PAN J B, *et al.*. Development of vacuum ultraviolet laser desorption/ionization single-cell mass spectrometry imaging instrument[J]. *Chinese Journal of Applied Chemistry*, 2024, 41(1): 100-108. (in Chinese).
- [25] FANG X Y, REN H R, LI K Y, *et al.*. Nanophotonic manipulation of optical angular momentum for high-dimensional information optics[J]. *Advances in Optics and Photonics*, 2021, 13(4): 772-833.
- [26] LI N N, LAI Y H, LAM S H, *et al.*. Directional control of light with nanoantennas[J]. *Advanced Optical Materials*, 2021, 9(1): 2001081.
- [27] PARK J, JEONG B G, KIM S I, *et al.*. All-solid-state spatial light modulator with independent phase and amplitude control for three-dimensional LiDAR applications[J]. *Nature Nanotechnology*, 2021, 16(1): 69-76.
- [28] SAVAGE N. Digital spatial light modulators[J]. *Nature Photonics*, 2009, 3(3): 170-172.
- [29] GUO Y J, GUO Y H, LI C S, *et al.*. Integrated optical phased arrays for beam forming and steering[J]. *Applied Sciences*, 2021, 11(9): 4017.
- [30] HE J W, DONG T, XU Y. Review of photonic integrated optical phased arrays for space optical communication[J]. *IEEE Access*, 2020, 8: 188284-188298.
- [31] ROSEN J, ALFORD S, ALLAN B, *et al.*. Roadmap on computational methods in optical imaging and holography[J]. *Applied Physics B*, 2024, 130(9): 166.
- [32] FOREMAN M R, TÖRÖK P. Computational methods in vectorial imaging[J]. *Journal of Modern Optics*, 2011, 58(5-6): 339-364.
- [33] RESHEF O, DE LEON I, ALAM M Z, *et al.*. Nonlinear optical effects in epsilon-near-zero media[J]. *Nature Reviews Materials*, 2019, 4(8): 535-551.
- [34] MORIMOTO T, NAGAOSA N. Topological nature of nonlinear optical effects in solids[J]. *Science Advances*, 2016, 2(5): e1501524.
- [35] YANG YJ, ZHAO Q, LIU L L, *et al.*. Manipulation of orbital-angular-momentum spectrum using pinhole plates[J]. *Physical Review Applied*, 2019, 12(6): 064007.
- [36] MA L, CHEN C, ZHAN Z J, *et al.*. Generation of spatiotemporal optical vortices in ultrashort laser pulses using rotationally interleaved multispirals[J]. *Optics Express*, 2022, 30(26): 47287-47303.
- [37] CAO H, WANG G Y, ZHANG L C, *et al.*. Reflective optical vortex generators with ultrabroadband self-phase compensation[J]. *Advanced Photonics Nexus*, 2023, 2(2): 026009.
- [38] WANG Z Y, ZHANG H, LIU X H, *et al.*. Cascaded liquid crystal holography for optical encryption[J]. *Chinese Optics Letters*, 2023, 21(12): 120003.
- [39] WANG G Y, CAO H, GUO ZH H, *et al.*. All-liquid-crystal and full-visible-band tunable polarimetry[J]. *Advanced Photonics Nexus*, 2025, 4(2): 025001.

Author Biographics:



MA Li (1990—), male, born in Changzhi, Shanxi Province, Ph.D., Lecture. He obtained his Ph.D. from Shandong Normal University in 2018 and completed his Postdoctoral Research Fellow at University of Otago in New Zealand in 2021. His research primarily focuses on optical modulations and ultrafast optics. E-mail: mali9001@126.com



ZHAO Bo (1986—), male, born in Changzhi, Shanxi Province, Ph.D., Professor, Master's supervisor. He obtained his Ph.D. from the Institute of Modern Optics at Nankai University in 2015. In 2018, he served as a post doctor and completed his postdoctoral research fellow at the China-US Joint Photon Laboratory under the guidance of GUO Chun-Lei at the Changchun Institute of Optics, Fine Mechanics and Physics, Chinese Academy of Sciences. His research primarily focuses on femtosecond laser micro-nano processing. E-mail: zy828522@163.com

《光学 精密工程》(半月刊)

- 中国光学开拓者之一王大珩院士亲自创办的新中国历史最悠久的光学期刊
- 现任主编为国家级有突出贡献的青年科学家曹健林博士
- Benjamin J Eggleton, John Love 等国际著名光学专家为本刊国际编委

《光学 精密工程》主要栏目有现代应用光学(空间光学、纤维光学、信息光学、薄膜光学、光电技术及器件、光学工艺及设备、光电跟踪与测量、激光技术及设备);微纳技术与精密机械(纳米光学、精密机械);信息科学(图像处理、计算机应用与软件工程)等。

- * 美国工程索引 EI 核心期刊
- * 中国出版政府奖期刊提名奖
- * 中国精品科技期刊
- * 中文核心期刊
- * 百种中国杰出学术期刊
- * 中国最具国际影响力学术期刊

主管单位:中国科学院

主办单位:中国科学院长春光学精密机械与物理研究所

中国仪器仪表学会

地址:长春市东南湖大路 3888 号

邮编:130033

电话:0431-86176855

传真:0431-84613409

电邮:gxjmgc@sina.com

网址: <http://www.eope.net>

定价:100.00 元/册